Catalysis Letters
https://doi.org/10.1007/s10562-018-2422-4

Amorphous Cr/SiO_2 Materials Hydrothermally Treated: Liquid Phase Cyclohexanol Oxidation

José Feliciano Miranda[1] · Pablo M. Cuesta Zapata[1] · Elio E. Gonzo[2] · Mónica L. Parentis[2] · Lilian E. Davies[1] · Norberto A. Bonini[1]

Received: 1 February 2018 / Accepted: 13 May 2018

Abstract

Amorphous $Cr–SiO_2$ materials were synthesized by the sol–gel method and hydrothermally treated at temperatures between 150 and 220 °C. These materials were used as catalysts for cyclohexanol oxidation with H_2O_2 as oxidant and CH_3CN as a solvent. They were responsible for the decomposition of H_2O_2, which triggers, by a free radical mechanism in the homogeneous phase, the oxidation or degradation of the hydrocarbon chain. Metal leaching causes a drop in catalytic activity when the material is recycled. Studies on the hydrothermal treatment effect on the leaching process have demonstrated that the higher the hydrothermal treatment temperature, the higher the metal/support interaction, leading to a diminution of the leaching process. Under mild reaction conditions, and using TBHP as oxidant, leaching was reduced, and improvements were obtained on the selectivity towards the formation of cyclohexanone. The use of these catalysts in the oxidation of verbenol, an allylic alcohol, showed a significant increase in the substrate conversion and in the selectivity to carbonyl derivative formation.

Graphical Abstract

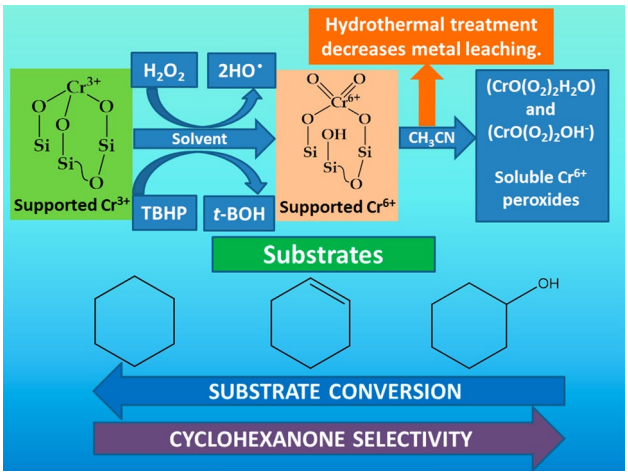

Keywords Cr/SiO_2 · Cyclohexanol · H_2O_2 · TBHP · Cyclohexanone · Hydrothermal treatment

1 Introduction

Cyclohexanone production is a process of great importance in the chemical industry. Annually, millions of tons of cyclohexanone are produced mostly for the synthesis of adipic acid and caprolactam, main precursors for the manufacture of Nylon-6 and Nylon-66 [1–5]. Cyclohexanone also

✉ Norberto A. Bonini
bonini@exa.unsa.edu.ar

Extended author information available on the last page of the article

Published online: 23 May 2018

finds application as additive and solvent in a wide variety of products, from insecticides to herbicides and pharmaceuticals products, paints, dyes, lacquers, varnishes and as homogenizer and stabilizer for soaps, among other minor applications and as a precursor in organic synthesis [6, 7].

In the synthesis process of adipic acid, cyclohexanone is produced by oxidation of cyclohexane with air, in the presence of cobalt naphthenate as a homogeneous catalyst and boric acid to stabilize the oxidation mixture [8, 9]. The final product is a mixture of cyclohexane (C–H), cyclohexanol (C–OL), cyclohexanone (C-ONE) and cyclohexyl hydroperoxide (C-HP), been the last the intermediate in the oxidation process. The unreacted C–H is distilling off and recycling while the low-volatile liquids, mainly C-OL and C-ONE, are purified by distillation leading to a mixture known as KA (ketone + alcohol) oil. The whole process is extremely costly as a consequence of the high temperatures (145–165 °C) and high O_2 pressures (1–2 Mpa) required. In this process, the C–H conversion is kept low (< 10%) to avoid over-oxidation of cyclohexanone and excessive waste production [6, 8, 10, 11].

Another industrial process for the production of cyclohexanone is the gas phase dehydrogenation of cyclohexanol in the presence of a heterogeneous copper catalyst [7, 12–15]. In this process, with the aim of having conversions close to 60 and 99% selectivity to cyclohexanone, a temperature of 260 °C [12, 14, 15] is used which causes loss of activity over time due to sintering. As a result, there is an increasing interest in developing new liquid phase oxidation processes exhibiting operative advantages such as mild conditions of reaction and the use of "soft" oxidants such as molecular oxygen, hydrogen peroxide or *ter*-butyl hydroperoxide (TBHP). However, these homogeneous liquid phase oxidations also need the presence of soluble transition metal complexes which cause damage to the environment; compelling their replacement by heterogeneous catalysts, which are easier to separate, recover and recycle [7, 16].

Between heterogeneous catalysts suitable for this reaction and obtained from supported transition metals [17, 18], chromium is particularly attractive due to its wide variety of oxidation states. In fact, chromium/silica catalysts were probed for cycloalkane liquid phase oxidations [6, 10, 16, 18–22], where the activity was ascribed to the presence of the redox pair Cr^{3+}/Cr^{6+} [19]. Although Adam et al. [10] and Sakthivel et al. [6] have synthesized Cr/SiO_2 catalysts with very high catalytic activity, these authors also have reported the leaching of chromium species into the reaction mixture, becoming the reaction carried out partially into the homogeneous phase. Chromium leaching seems to be a recurring problem with this kind of materials [16, 20, 23], especially when using TBHP or H_2O_2 in the presence of polar solvents such as water or acids [24]. Thus, the development of heterogeneous, highly stable, and active catalysts for the selective oxidation of organic compounds is one of the main challenges for the environmentally "green" catalysis.

The sol–gel method for preparing catalysts is suitable for incorporating metal ions homogeneously dispersed into the silica structure. However, the stability of these metal ions is not enough to avoid leaching into the liquid phase [6, 16, 20]. Recently, our research group has reported the synthesis of Cr–SiO_2 catalysts by sol–gel technique followed by hydrothermal treatment [25–27] up to 220 °C. It was observed a progressive incorporation of Cr^{3+} ions in the silica network as the hydrothermal temperature increases from 120 to 220 °C. The nature of Cr–SiO_2 interaction was studied by techniques such as XPS, UV–Visible DRS, and adsorption of probe molecules followed by FTIR analysis. It was shown that chromium species are incorporated into the silica framework by forming chromasiloxane rings with hydrothermal treatment [28–30]. It was also showed that even small amounts of Cr^{3+} coordinative unsaturated sites are just enough to produce the dehydration of cyclohexanol in gas phase diminishing the selectivity to cyclohexanone [28–30]. Therefore, the sol–gel technique combined with hydrothermal treatments seem to be an interesting method for preparing materials with Cr^{3+}/Cr^{6+} centers, highly dispersed, and stable from leaching into the liquid phase.

In the present work, the catalytic activity of the chromium catalysts, prepared by the sol–gel technique and hydrothermally treated, was evaluated. They were tested against the oxidation of different substrates, mainly cyclohexanol, to cyclohexanone in the liquid phase, using H_2O_2 as oxidizer and acetonitrile as solvent. The effect of hydrotreatment temperature on catalytic activity was studied. For comparison, the behavior of the system when TBHP (70% in water) is used as an alternative oxidizing agent was analyzed. Finally, the behavior of verbenol, a cyclic allylic alcohol, was compared with that of cyclohexanol using H_2O_2 as the oxidizing agent.

2 Experimental

2.1 Catalysts Preparation

Tetraethyl orthosilicate (TEOS, Merck) was used as the silica source in all syntheses. It was mixed with ethanol (EtOH) (Merck 99.9%), stirred at 60 °C, and the pH adjusted to 9.5 with NH_4OH (Merck). Then, a solution of $Cr(NO_3)_3.9H_2O$ (ANEDRA > 98%) dissolved in an EtOH/H_2O (1:1 v/v) mixture was dropped, under stirring. The amount of chromium was the required to obtain a Cr/TEOS molar ratio of 0.06 and adequate to produce a 5% w/w of chromium on silica catalyst (5**SG**). The final mixture, (molar ratio of 1.0TEOS:225.0H_2O:30.3EtOH), was vigorously stirred for one hour and allowed to gel during 40 h. Portions of the gel

were autoclaved in a Teflon vessel at different temperatures (120–220 °C) for 24 h. After hydrothermal treatment, the solid product was filtered and washed; first with water and then with an EtOH/acetone (1/1) mixture to avoid deposition of soluble chromium salts during drying. Finally, samples were dried in air up to 110 °C. Materials were assigned as $5\mathbf{SG}_{xxx}{}^{yyy}$ where xxx is the hydrotreatment temperature and yyy the highest treatment temperature in air. Non-hydrotreated samples were denoted as $5SG_{nHT}$.

2.2 Sample Characterization

2.2.1 Textural Characterization

Adsorption–desorption isotherms were carried out in a Micromeritics ASAP-2020 sorptometer, employing N_2 as the adsorbent. Specific surface area (S_{BET}) was calculated using the standard BET method. The pore size distributions were determined from the adsorption branch of the isotherms using the BJH method.

2.2.2 Atomic Absorption Spectroscopy

Chromium loading was determined by atomic absorption (AA) spectroscopy, with a GBC 904 AA spectrometer, after dissolving the samples with HF.

Leaching tests on the liquid supernatant were performed, at 70 °C, after 7 h of contacting either the catalyst with substrate and solvent or the catalyst with the substrate, solvent, and oxidant. The same amount of liquid sample was used for leaching tests as well as for catalytic activity assays.

2.2.3 UV–Vis Diffuse Reflectance Spectroscopy (DRS)

A GBC-918 equipment, with a $BaSO_4$ diffuse reflectance sphere as a reference, was used in the 190–900 nm range for the UV–Vis diffuse reflectance analysis. The spectra were determined over finely grounded materials gently compacted into the sample compartment of the spectrophotometer.

2.2.4 FTIR-2,6-lutidine Adsorption

The FTIR spectra were recorded on a Spectrum GX-FTIR Perkin-Elmer Spectrophotometer. FTIR measurements in vacuum and 2,6-lutidine (Lu) adsorption were carried out over a self-supporting wafer (20 mg approx.) in a cell with KRS-5 windows that allows vacuum (10^{-5} mmHg) and heating treatments "in-situ". Each sample was evacuated at different temperatures and the spectrum recorded (baseline). Gaseous Lu was introduced and left to equilibrate at its corresponding vapor pressure at room temperature (RT). After Lu adsorption, the cell was evacuated at different evacuation temperatures and the spectra recorded.

Difference spectra were obtained by subtracting the spectra of the pure sample (baseline spectrum) from those of the sample interacting with the adsorbed molecule after vacuum treatment. For quantitative determinations, the spectra were normalized using, as an internal standard, the overtones and combination bands in 2100–1800 cm^{-1} region.

2.3 Catalytic Activity

Catalytic activity tests were performed in an 18 mL flat bottom vial (Perkin Elmer) with a plastic cap and PTFE/silicone septum. A mixture of 10 mg of catalyst, 5 mL of solvent (acetonitrile or chlorobenzene), 5 mmol of cyclohexanol and 5 mmol of oxidant was introduced into the reactor. The reaction was carried out at 70 °C under stirring. The addition of the oxidizing agent (H_2O_2 30% or TBHP 70% in H_2O) was performed on aliquots at scheduled times (t = 0 and 2 h, 2 mmol, and t = 3, 4 and 6.5 h, 1 mmol). Aliquots of the reaction mixture (0.1 mL) were taken at different reaction times, filtered through a membrane filter (PTFE-0.45 μm), dissolved in acetonitrile and cooled at 0 °C (to ensure quickly quenching of the reaction) until chromatographic analysis. The concentration of reactants and products was determined by gas chromatography (GC) with a Hewlett Packard-5890 Series II gas chromatograph equipped with an HP-20 capillary column (L = 25 m, DI = 0.32 mm) and a flame ionization detector (FID) using chlorobenzene as internal standard (SI). Products and by-products of the reaction were identified by gas chromatography (Perkin Elmer Clarus 680) coupled to a mass detector (MS) (Perkin Elmer Clarus 600, Elite-5MS column, L = 30 m, DI = 0.32 mm) and their mass spectra compared with those in NIST 08 and Wiley 2010 libraries.

The H_2O_2 decomposition was determined by iodometric titration of aliquots taken off at different periods.

3 Results and Discussion

3.1 Characterization

3.1.1 N_2 Adsorption

Table 1 shows textural properties for 5SG samples determined from the N_2 adsorption–desorption isotherms: BET specific surface area (S_{BET}), mean pore diameter (D_P), and pore volume (V_{TP}).

Both the specific surface area (S_{BET}) and the pore volume (V_{TP}) decreased when the hydrotreatment temperature increased (Table 1). The pore diameter distribution (D_p) is narrow and centered around 43 Å for the sample without hydrotreatment ($5SG_{nHT}$). Hydrothermally treated samples developed a bimodal profile with a broad distribution

Table 1 5% Chromium content and textural properties of SG materials

Sample	S_{BET} ($m^2\ g^{-1}$)	V_{TP} ($cm^3 g^{-1}$)	D_P (Å)	% Cr (w/w) (*)
$5SG_{nHT}$	608	0.735	43	4.1 ± 0.1
$5SG_{150}$	240	0.358	18–34	4.5 ± 0.4
$5SG_{220}$	136	0.154	19–25	4.9 ± 0.4

(*) from AA analysis

characteristic of amorphous siliceous materials. Moreover, the chromium loading (Table 1), in all materials, was lower than the theoretical amount added because the non-anchored chromium was released by washing before drying (see "Experimental" section). On the other hand, the amount of chromium was lesser into the $5ME_{nHT}$ material than in the hydrotreated samples. This difference is attributed to the lower amount of water and surface hydroxyl groups present on hydrotreated materials as result of the S_{BET} decrease (Table 1). However, it must also consider that, under hydrothermal conditions, a partial solubility of the Si-oligomers occurs, leading to a consequent increase in the final chromium content.

3.1.2 UV–Vis Diffuse Reflectance Spectroscopy (DRS)

Cr^{3+} is a d^3 ion that presents three intense absorption bands, in the 200–900 nm spectral region, corresponding to three allowed electronic transitions. The $[Cr(H_2O)_6]^{3+}$ ion shows these bands centered at 580, 412 and 260 nm, and also a weak band as a shoulder at 680 nm corresponding to a spin-forbidden transition [31]. The $5SG_{nHT}{}^{110}$ material shows a shift of the 580 nm band toward higher wavelengths at 604 nm. This red shift is due to the presence of ammonia as ligand and the incorporation of Si–O groups in the outer coordination sphere of Cr^{3+} ions [27]. A shift of the two bands in the visible region to higher wavelengths, due to the effect produced by the hydrothermal-treatment, was observed (Fig. 1; Table 2). Thus, a gradual increase of the hydrotreatment temperature during the synthesis produces a gradual shift in the $^4T_{2g}(F) - {}^4A_{2g}(F)$ absorption band, from 604 nm ($5SG_{110}$) to 622 nm ($5SG_{220}$). This behavior must be justified by the formation of Si–O–Cr bonds. The shift was accompanied by a strong change in the relative intensities of the absorption bands. As a result, the ratio $R = (^4T_{2g} - {}^4A_{2g})/(^4T_{1g} - {}^4A_{2g})$ goes from 1, for $5SG_{nHT}{}^{110}$, to 2 for $5SG_{220}{}^{110}$ (Table 2; Fig. 1).

These changes reflect the distortion of the octahedral field produced by the incorporation of Cr^{3+} ions in the tetrahedral structure of silica. This distortion is related to the formation of strained chromium siloxane rings reported in the literature [28–30]. These Cr^{3+} ions constitute coordinative unsaturated (CU) centers. The calcination in air from 300 up to 450 °C of these materials produce the partial oxidation of the Cr^{3+} with the development of mono and polychromate Cr^{6+} species. Such a behavior was confirmed by the partial disappearance of the $(^4T_{2g} - {}^4A_{2g})$ and $(^4T_{1g} - {}^4A_{2g})$ bands and a strong increase of the Cr^{6+} metal to ligand charge transfer band into the 230–350 nm spectral region [27].

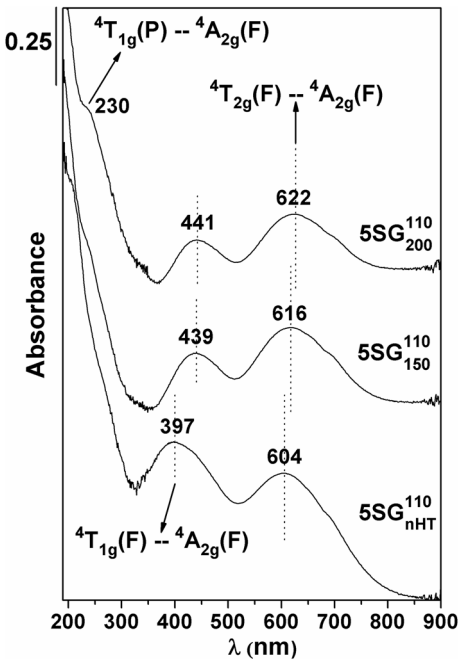

Fig. 1 DRUV–vis spectra obtained from samples prepared under different hydrothermal conditions: **a** $5SG_{nHT}{}^{110}$, **b** $5SG_{150}{}^{110}$, **c** $5SG_{220}{}^{110}$. The shoulder between 680 and 710 nm corresponds to a spin-forbidden transition

The resistance of Cr^{3+} to Cr^{6+} oxidation depends on the hydrotreatment. So, while after calcination at 450 °C in the $5SG_{nHT}$ materials almost all the Cr^{3+} signals disappear, these signals are evident on the $5SG_{220}{}^{450}$ material [27].

3.1.3 FTIR Study of 2,6-lutidine Adsorption

The presence of CU Cr^{3+} ions anchored to the silica surface produces Lewis acid centers, and their oxidation in air promotes the development of weak Brønsted sites [27]. The evolution of these acid centers was studied by FTIR through

Table 2 Electronic transitions of Cr^{3+} ions observed by DRUV–Vis spectroscopy

Sample	$^4T_{2g}(F) \rightarrow {}^4A_{2g}(F)$ (nm)	$^4T_{1g}(F) \rightarrow {}^4A_{2g}(F)$ (nm)	$R = I_{(620\ nm)}/I_{(425\ nm)}$
$5SG_{nHT}{}^{110}$	604	397	0.82
$5SG_{150}{}^{110}$	616	439	1.65
$5SG_{220}{}^{110}$	622	441	2.00

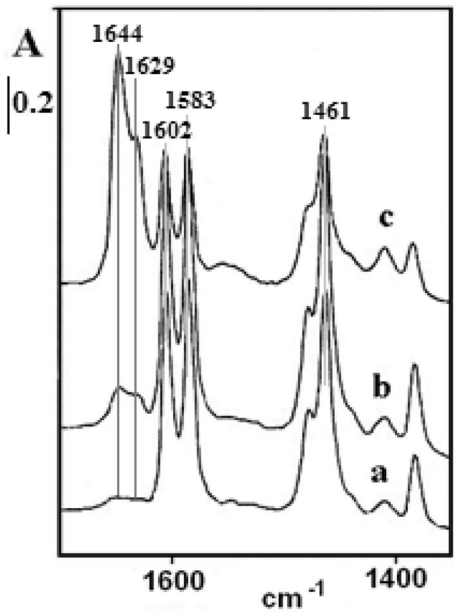

Fig. 2 Lu adsorbed on $5SG_{nHT}$ material calcined at: *a* 150 °C, *b* 350 °C, *c* 450 ºC

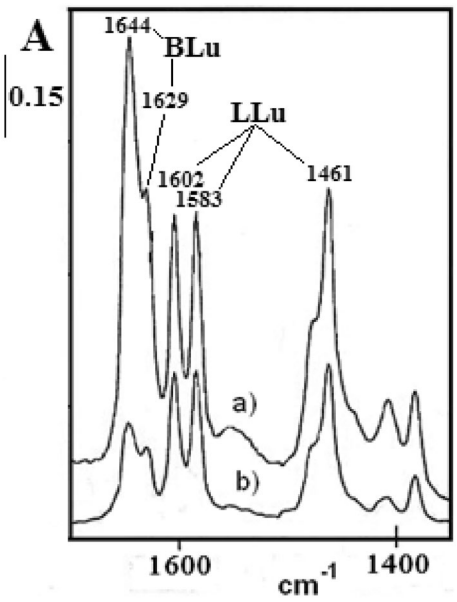

Fig. 3 BLu species developed over different 5SG materials calcined at 450 °C. *a* $5SG_{nHT}^{450}$, *b* $5SG_{220}^{450}$. The spectra were determined after evacuation for 30 min at room temperature

the adsorption of 2,6-lutidine (Lu) molecules. On $5SG_{nHT}^{110}$ materials previously evacuated at 250 °C, the Lu adsorption leads to the development of IR bands at 1602, 1583, 1475, 1461, 1408 and 1382 cm^{-1} (Fig. 2a). These bands are assignable to hydrogen-bonded lutidine (HBLu) and/or Lu interacting with Lewis acid sites (LLu). Discriminating between them is only possible by vacuum treatment. Therefore, while HBLu completely disappears in vacuum at 50 °C, removing LLu requires vacuum treatment higher than 100 °C.

While in samples heated in N_2 or in vacuum up to 450 °C before the adsorption of Lu the nature of the adsorbed species don´t change, the Lu adsorption on materials calcined in air leads to the development of a new band at 1644 cm^{-1} with a shoulder at 1629 cm^{-1} (Fig. 2b, c). These bands correspond to the appearance of a protonated 2,6-lutidinium ion, formed by interaction of Lu with Brønsted acid sites (BLu). The amount of BLu depends on both the previous hydrothermal treatment and the temperature of in-air calcination. The rise of the calcination temperature increases the amount of BLu at expense of Lewis species. Therefore, on $5SG_{nht}$ calcined at 450 °C the most intense bands observed correspond to BLu (Fig. 2c). These BLu species resist the vacuum treatment up to 100 °C. From these results, we conclude that LLu is related to Cr^{3+} ions, while BLu appears when Cr^{6+} forms by calcination.

After calcination, on hydrothermally treated samples ($5SG_{220}^{450}$) the relative amount of Brønsted to Lewis acid sites is markedly lower than in non-hydrothermally treated materials ($5SG_{nHT}^{450}$) (Fig. 3). The lower amount of Brønsted acid centers coincides with a greater resistance toward oxidation of Cr^{3+} ions on hydrothermally treated samples as it was observed by DRUV–Vis experiences [27].

To verify whether Brønsted centers correlates to the Cr^{6+} presence and their leachability, a $5SG_{220}^{450}$ sample, which after calcination in air developed a light yellow color, was washed with acetone and ethanol. After washing and drying in air at room temperature, a self-supported wafer of this material was made; it was evacuated at 150 °C into the FTIR cell and put in contact whit Lu vapors. Figure 4 shows that only LLu/HBLu bands formed on this material after interaction with Lu. A new heating of the washed sample in air at 450 °C (Fig. 4b) shows the development of new Brønsted acid centers at the expense of the Lewis ones. These results let us conclude that the development of Brønsted centers is directly related to the Cr^{6+} species formed during calcination in air.

Conversely, the intensity of the BLu bands decreased when the sample, before the adsorption of Lu, was treated in vacuum at increasingly higher temperatures (Fig. 4c, d). The color of the sample turns progressively to dark blue-green instead of the yellow color observed on the oxidized one. So, in vacuum at 450 °C, almost all Cr^{6+} transforms to Cr^{3+}. This behavior shows that the Cr^{3+}–Cr^{6+} redox process on the Cr/SiO_2 system is reversible. The amount of both ions depends on the temperature and the oxidative character of the atmosphere used during calcination, as well as on the presence of an oxidizing agent (H_2O_2 or TBHP) in the liquid phase as will be discussed later.

From the above results and those reported in previous papers [25–27], we can conclude that Cr^{3+} species were the

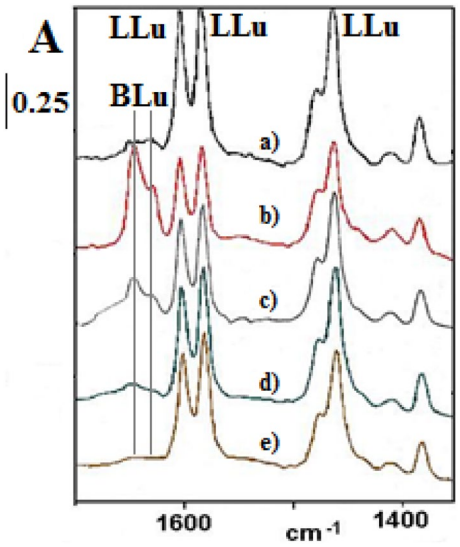

Fig. 4 Difference spectra of Lu adsorbed on $5SG_{220}^{450}$ materials after different treatments: *a* $5SG_{220}^{450}$ washed with acetone/EtOH, *b* sample *a* calcined in air up to 450 °C; (*c*–*e*) Lu adsorption on sample *b* after treatment in vacuum (1 h – 10^{-5} mmHg) at 250, 350 and 450 °C successively

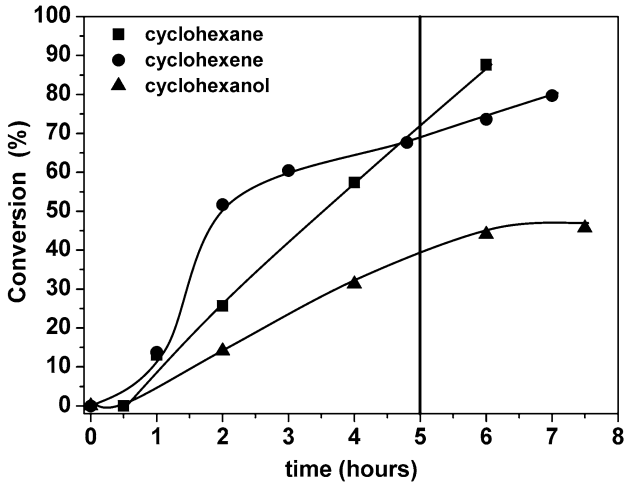

Fig. 5 Oxidation of different substrates in the presence of H_2O_2 on Cr/SiO_2 catalyst. Temperature: 70 °C. Solvent: CH_3CN (5 mL). Catalyst: $5SG_{150}^{110}$ (10 mg). Substrate: 5 mmol. Oxidizing agent: H_2O_2 (30%) added at programmed stages to 10 mmol (molar ratio R = substrate/H_2O_2 = 0.5) except for cyclohexanol for which R = 1

only one into the catalyst samples dried at 110 °C, whereas in samples treated at temperatures higher than 110 °C, both Cr^{3+} and Cr^{6+} species were present. Similar results were obtained over Cr-MCM-41 materials on which the relative amount of both species was quantified by XPS [25, 26].

All the above characterization results let to conclude that hydrothermal treatment enhances the incorporation of Cr^{3+} into the silica structure, through the Si–O–Cr bonds formation, avoiding the leaching and also the formation of either dichromate or polychromate polymeric species [25–27]. The X-ray diffraction profiles of 5SG materials (not shown) established the absence of crystalline species, even after calcination in air up to 450 °C. The last because of the low loading and high chromium dispersion. The superficial chromium species formed, studied by FTIR of chemisorbed pyridine (Py) [25, 27] and 2,6-lutidine (Lu), allowed establishing the presence of highly unsaturated Cr^{3+} centers that partially develop, after calcination in air at 450 °C, Cr^{6+} centers associate to the presence of Brønsted acid sites.

3.2 Catalytic Activity in Liquid Phase

3.2.1 Oxidation of Different Substrates

The oxidation reaction of cyclohexane, cyclohexene, and cyclohexanol to cyclohexanone was studied to investigate the catalytic activity of the $5SG_{150}^{110}$ materials. Results are shown in Fig. 5.

After 5 h of reaction, conversions near to 70% were observed for the cyclohexane and cyclohexene substrates. For cyclohexane, conversion exceeded 90% after 6 h with selectivity to cyclohexanol and/or cyclohexanone lower than 10%. The main by-products were short chain carboxylic acids and CO_2. This behavior agrees with the results obtained by Adam et al. [10] on Cr/SiO_2 catalyst prepared by the impregnation method, in which the major products were cyclohexanol, cyclohexanone, adipic acid and decomposition products of the hydrocarbon chain, such as valeric, acetic and butyric acids, among others.

When the molar ratio R, between the substrate and oxygen peroxide, was equal to 2, the process resembles the organic substrates decomposition with H_2O_2 in an acid medium in the presence of Fe^{2+} salt (Fenton process). In our case, the high tendency to chain degradation and low selectivity to carbonyl derivatives is attributed to the strong surface acidity of 5SG catalyst and the chromium ability to generate $HO^{\bullet}$ radicals from H_2O_2 (Scheme 1).

Like cyclohexane, cyclohexene also suffers rapid oxidation in the presence of H_2O_2. Thus, after 3 h of reaction (Fig. 5), more than 60% of the substrate was converted to degradation products. The oxidation of cyclohexene with H_2O_2 using polar solvents such as acetonitrile or H_2O is one of the ways commonly chosen for the direct preparation of adipic acid. The reaction mechanism involves the formation of intermediates species such as cyclohexene oxide, 1,2-cyclohexanediol, 2-hydroxycyclohexanone and adipic anhydride [16, 32,

$$Cr^{3+} + 3\ H_2O_2 \rightleftharpoons Cr^{6+} + 3\ HO\cdot + 3\ HO^-$$

Scheme 1 H_2O_2 decomposition on Cr/SiO_2 catalysts

33]. Among the oxidation products obtained with $5SG_{150}^{110}$ catalyst, small amounts of cyclohexene oxide, 1,2-cyclohexanediol, and 2-hydroxycyclohexanone but not anhydride or adipic acid were detected by gas chromatography and mass spectrometry.

On the other hand, a low oxidation reaction rate and selectivity to cyclohexanone higher than 30% were observed when cyclohexanol was used as the substrate. In this case, by GC-MS analysis, cyclohexanone was identified as the main product, along with 3-hydroxycyclohexanone, 4-hydroxycyclohexanone, 2-hydroxycyclohexanone and 2-cyclohexenone as minor products. These results allow proposing that after the oxidation to cyclohexanone, the formation of more oxygenated by-products follow the path to ring opening. In the absence of the catalyst, the oxidation of these substrates showed very low conversions. So, the presence of the catalyst was essential to trigger off the H_2O_2 decomposition.

From these results, and to have a better insight of the process, new experiences were programmed to investigate the effect of different variables on the activity and selectivity of 5SG catalysts over the cyclohexanol oxidation in the presence of acetonitrile as solvent. This system is interesting to study since the little knowledge of this reaction performed in non-halogenated solvents [19].

3.2.2 Reaction Temperature Effect on the Cyclohexanol Conversion

The effect of the reaction temperature on the total conversion (C_{C-OL}) and selectivity to cyclohexanone (S_{C-ONE}) over the $5SG_{150}^{110}$ material, hydrothermally prepared at 150 °C, was determined. As expected, reaction proceeds faster at 70 °C than at 50 °C. At 50 °C and after 6 h of reaction, the C_{C-OH} was near 10% with null selectivity to cyclohexanone (Fig. 6, right). Meanwhile, at 70 °C, the C-OH conversion reaches approximately 45% and selectivity towards cyclohexanone 25%. Figure 6, shows that, at the beginning and until two hours of reaction at 70 °C, when the concentration of hydrogen peroxide is high, the degradation of the hydrocarbon chain is important with S_{C-ONE} near 10%. This behavior suggests that degradation and oxidation reactions run through independent paths not being cyclohexanone an intermediate in the chain degradation reaction.

3.2.2.1 The Effect of Catalyst Amount Loaded Figure 7, shows the effect of the amount of catalyst added on C_{C-OH} and also in the S_{C-ONE}. In the absence of the catalyst, the reaction rate is very low ($C_{C-OH} = 5\%$). After 7 h, cyclohexanone was not found between the oxidation products; it was detected after 23 h of reaction with selectivity close to 7%. This behavior reflects the role of the catalyst in the decomposition of the oxidizing agent. Accordingly, monitoring H_2O_2 decomposition in the absence of the substrate shows that the 10 mmol of H_2O_2 fully decomposed over the $5SG_{150}^{110}$ catalyst after 5 h of reaction at 70 °C.

Figure 7 also shows that different amounts of loaded catalytic material produce almost the same C_{C-OL} and negligible differences in S_{C-ONE}. These results seem to reflect that, although the catalyst plays a leading role in the decomposition of H_2O_2, it induces, through a free radical mechanism in homogeneous phase (see Scheme 1 above), the oxidation and the subsequent degradation of the hydrocarbon chain. Other authors [10] have also reported similar results.

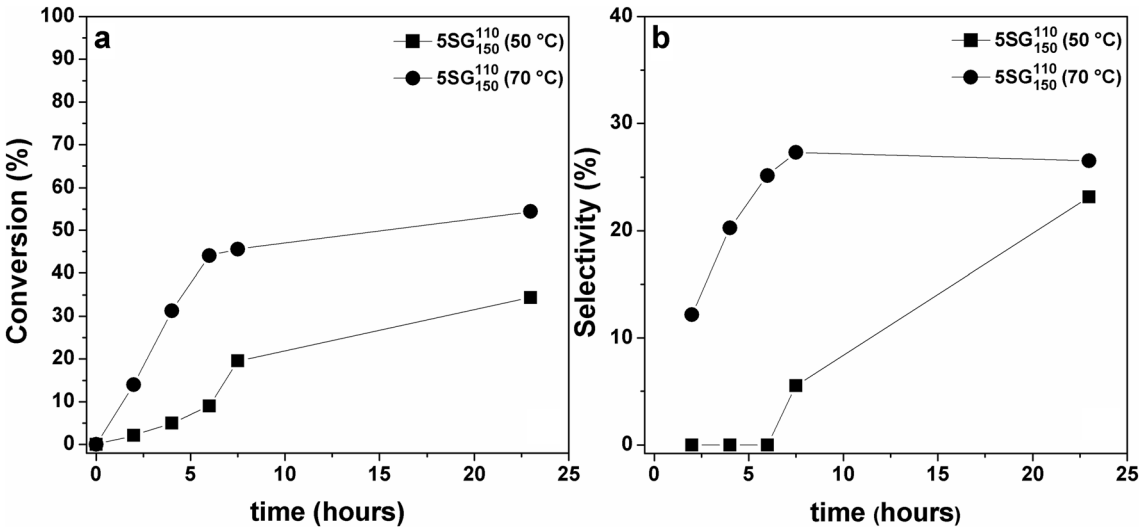

Fig. 6 Effect of reaction temperature on **a** cyclohexanol conversion and **b** cyclohexanone selectivity. Catalyst: $5SG_{150}^{110}$ (10 mg). Solvent: CH_3CN (5 mL). Substrate: 5 mmol. Oxidizing agent: H_2O_2 (0.7 mL, 30%). (R = 1)

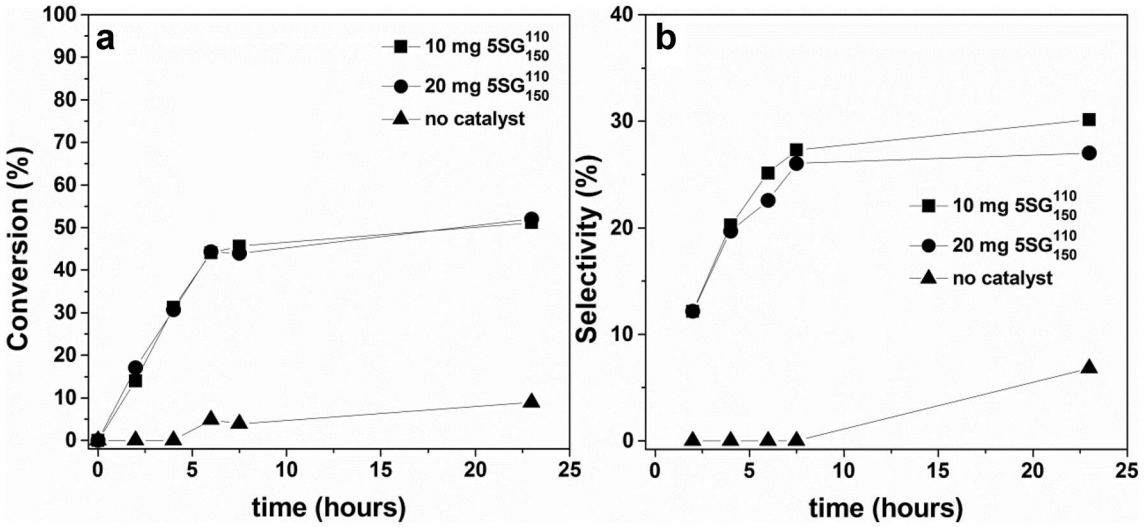

Fig. 7 Effect of the amount of catalyst loaded. **a** Cyclohexanol conversion. **b** Cyclohexanone selectivity. Temperature: 70 °C. Catalyst: $5SG_{150}^{110}$ (10 mg/ 20 mg). Solvent: CH_3CN (5 mL). Substrate: cyclohexanol (5 mmol). Oxidizing agent: H_2O_2 (0.7 mL, 30%). (R = 1)

3.2.2.2 Catalyst Lifetime and Number of Cycles Three cycles of reuse were carried out to analyze the lifetime and reusability of the catalyst. After each cycle, the Cr/SiO_2 material was filtered, washed with hot acetonitrile and added to a fresh reaction mixture for running a new activity test.

It was observed a loss of catalytic activity as the number of cycles increased (Fig. 8a). However, the loss of activity was not accompanied by a significant change to cyclohexanone selectivity (Fig. 8b).

The slight drop in C_{C-OL} conversion through the successive cycles suggests that a fraction of chromium ions are lost by the leaching process. Took into account the careful washing of the solid done after each cycle to ensure the complete removal of lixiviated metal, we conclude that hydrogen peroxide favors the leaching of the supported Cr ions by Cr^{6+} formation. These results are coincident with that observed by Lu-adsorption FTIR (Fig. 4) were the Cr^{+3} to Cr^{6+} oxidation, when catalysts are heated in air, was produced.

This comportment coincides with the violet coloration acquired by the reaction medium after addition of hydrogen peroxide that disappears as the reaction proceeds. The same but more intense coloration was observed when a chromium(III) salt was dissolved in acetonitrile in the presence of hydrogen peroxide and heated up to 70 °C. This behavior is related to the formation of the soluble Cr^{6+} peroxides, like the blue $(CrO(O_2)_2H_2O)$ and violet

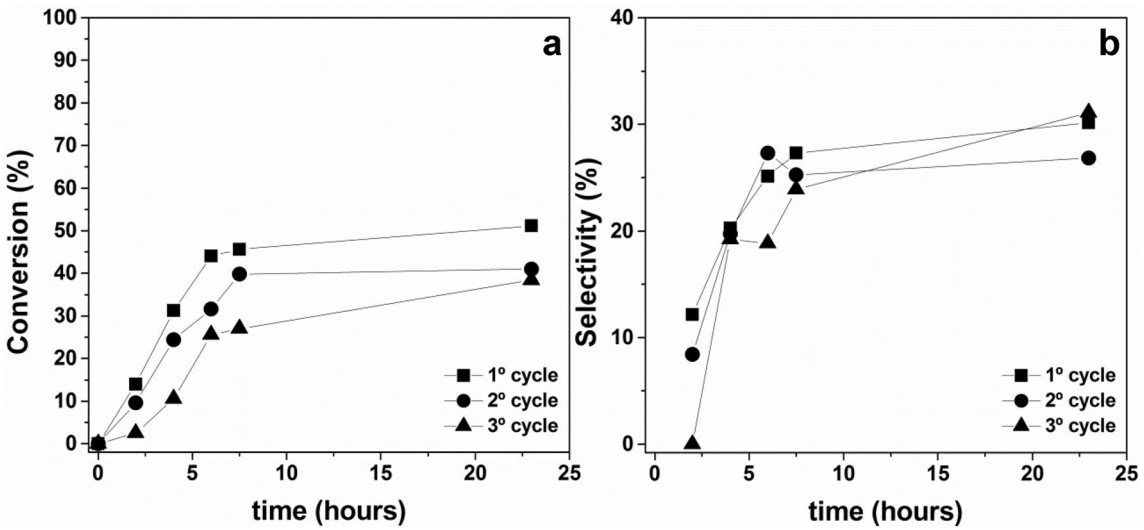

Fig. 8 Behavior as a function of the number of cycles. **a** Cyclohexanol conversion. **b** Cyclohexanone selectivity. Temperature: 70 °C. Solvent: CH_3CN (5 mL). Catalyst: $5SG_{150}^{110}$ (10 mg). Substrate: cyclohexanol (0.5 mL). Oxidizing agent: H_2O_2 (0.7 mL, 30%)

$(CrO(O_2)_2OH^-)$ peroxides [34]. Both complexes readily decompose to form Cr(III) ions, in acid media.

3.2.2.3 Homogeneous Phase Reaction To investigate the leaching of chromium ions into the homogeneous phase, the catalytic activity was evaluated by removing the catalyst after one-hour reaction [22]. Figure 9 shows a comparison between the reaction performed in the presence of $5SG_{nHT}{}^{110}$ catalyst and the reaction when the catalyst was removed after one hour of reaction. For comparison, and considering that the leaching and reusability of the $5SG_{150}{}^{110}$ catalyst were determined previously (Fig. 8), the catalyst with no hydrothermal treatment was chosen since it presents the weakest metal-support interaction and consequently it is the most susceptible to leaching [25–27].

Figure 9 shows that, after removing the catalyst, the reaction proceeds in the homogeneous phase with almost identical conversion to that obtained in the presence of the catalyst. On the other hand, the selectivity to carbonyl derivative decreases when the reaction is completed in homogeneous phase. This behavior confirms that hydrogen peroxide initiates the reaction by oxidation of surface Cr^{3+} ions to form soluble Cr^{6+} peroxides. They catalyze the homogeneous phase reaction until the disappearance of the oxidizing agent promoting the degradation of the cyclic chain. So, the catalyst presence exerts an improving effect on the selectivity to the carbonyl derivative.

3.2.2.4 Leaching Tests To determine the leaching degree of chromium ions during the progress of the reaction, we carried out some experiments using CH_3CN as solvent at 70 °C for 7 h, both in the presence and absence of H_2O_2.

Table 3 shows the percent of chromium leached out based on the total chromium content of the catalyst (Table 1). It is observed that, regardless of hydrothermal treatment, without the oxidizing agent metal leaching does not occur due to the insolubility of Cr^{3+} in CH_3CN. By contrast, in the presence of H_2O_2, the amount of metal leached from $5SG_{nHT}$ material was 73% after the first cycle, reaching 95% after the second one. Note that the higher was the hydrothermal treatment temperature, the lower the metal leached out. Consequently, for the hydrothermally treated material at 220 °C ($5SG_{220}{}^{110}$), the leaching was only 12% and 18% after the first and second cycle, respectively. An intermediate behavior was observed for the material hydrotreated at 150 °C; being the total chromium leached out 29 and 49% in the first and second washings, respectively. The leaching behavior confirms the previously reported [25–27] regarding the increase of the metal-support interaction with the rise of the hydrothermal treatment temperature. In all cases, the leaching process was accompanied by the development of a violet coloration whose intensity depends on the metal

Table 3 Total chromium loss in leaching tests

Sample	CH_3CN[a]		$CH_3CN + H_2O_2$[a]	
	First wash (%)	Second wash (%)	First wash (%)	Second wash (%)
$5SG^{110}{}_{nHT}$	0	0	73	95
$5SG^{110}{}_{150}$	0	0	29	49
$5SG^{110}{}_{220}$	0	0	12	18

[a]Washing made after 7 h at 70 °C under stirring

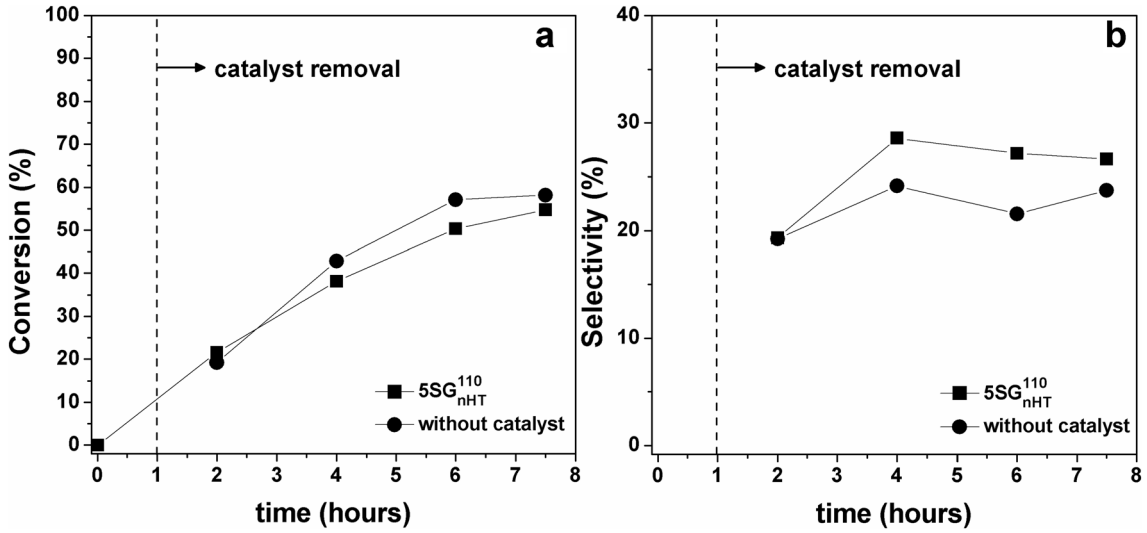

Fig. 9 Comparison of the system with $5SG_{nHT}{}^{110}$ catalyst and the same system one hour after removing the catalyst. **a** Cyclohexanol conversion. **b** Cyclohexanone selectivity. Temperature: 70 °C. Solvent: CH_3CN (5 mL). Catalyst: $5SG_{nHT}{}^{110}$ (10 mg). Substrate: cyclohexanol (0.5 mL). Oxidizing agent: H_2O_2 (0.7 mL, 30%)

concentration in solution, given support to the presence of Cr^{6+} peroxide species into the solvent.

3.2.2.5 Effect of hydrothermal treatment temperature The cyclohexanol conversion and cyclohexanone selectivity on hydrothermally treated materials at different temperatures (nHT, 150 °C, 220 °C) are depicted in Fig. 10. Figure 10a shows that increasing the hydrotreating temperature reduces both the catalytic activity (total cyclohexanol conversion) and selectivity towards cyclohexanone. After 7 h of reaction in presence of the material without hydrotreatment ($5SG_{nHT}{}^{110}$) the C_{C-OH} was 60% approximately and S_{C-ONE} around 25%. Under the same reaction conditions, the $5SG_{220}{}^{110}$ material gave a 30% conversion and cyclohexanone selectivity as low as 10%. The $5SG_{150}{}^{110}$ material (hydrothermal temperature of 150 °C) showed an intermediate behavior.

On the other hand, the initial reaction rates values (Fig. 11) for both total C-OH conversion (mmol of C-OH h^{-1} m^{-2} mol Cr^{-1}) and C-ONE formation (mmol of C-ONE h^{-1} m^{-2} mol Cr^{-1}) show a volcano shape, with the $5SG_{150}{}^{110}$ material displaying the maximum value. This maximum is due to the competition between the homogeneous reaction in the liquid face and the heterogeneous reaction on the solid surface.

Besides, the difference observed between r_{C-OH} and r_{C-ONE} resembling selectivity (Fig. 10b) must be interpreted in terms not only of the amount of Cr^{6+} leached off but also as the consequence of the acidity changes (amount and strength) occurring into the surface of 5SG materials by the hydrotreatment.

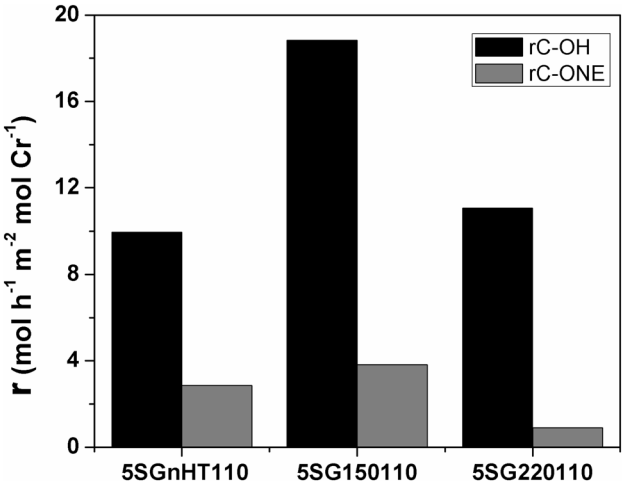

Fig. 11 Initial reaction rates for 5SG materials determined by the conversion at 4 h of reaction

So, the higher the hydrotreatment temperature, the stronger the Cr^{3+}/support interaction and its resistance to being leached out, diminishing the availability of Cr^{6+} species in solution for the redox process (Fig. 10a). However, the strong metal/support interaction increases the amount of coordinative unsaturated Cr^{+3} centers and hence the Lewis superficial acidity [27]. These centers promote the opening of the cyclic hydrocarbon chain and its later degradation. Both effects produce a maximum in the reaction rate (Fig. 11) and therefore, reduction of leaching degree and acidity increase, result in a lower reactivity and a lower selectivity to carbonyl derivatives for the $5SG_{220}{}^{110}$ material. A similar effect was reported in the oxy-dehydrogenation

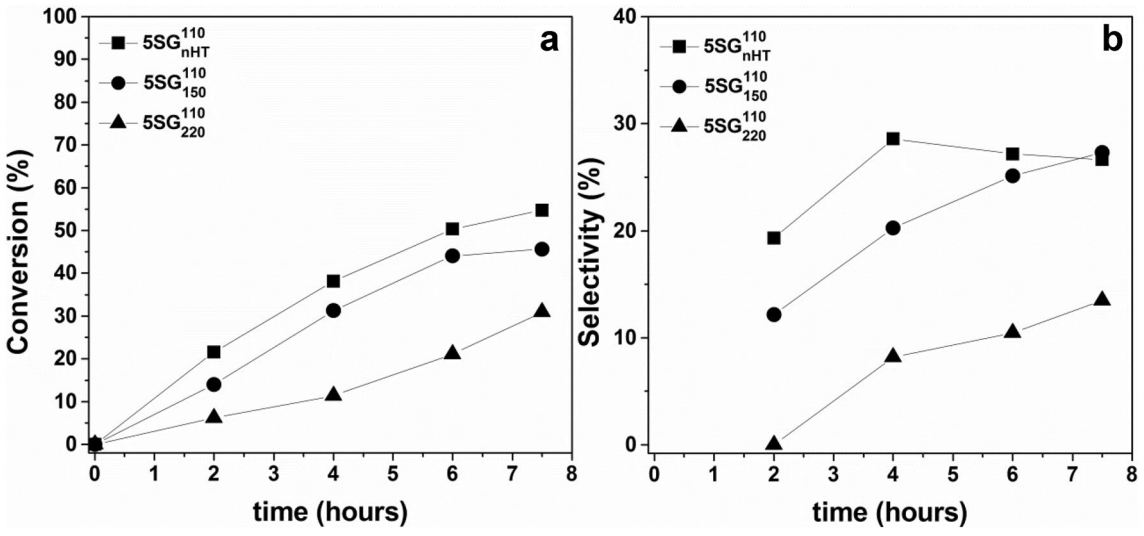

Fig. 10 Influence of hydrothermal treatment temperature. **a** Cyclohexanol conversion. **b** Cyclohexanone selectivity. Temperature: 70 °C. Solvent: CH_3CN (5 mL). Catalyst: 10 mg. Substrate: cyclohexanol (0.5 mL). Oxidizing agent: H_2O_2 (0.7 mL, 30%)

of alcohols (2-propanol and C–OH) in the gas phase [27]; where materials without hydrothermal treatment showed greater selectivity towards the carbonyl derivatives than those materials prepared by hydrothermal treatment at 220 °C. So, the latter ones showed, in the gas phase at 280 °C, almost exclusively dehydrating activity over 2-propanol and cyclohexanol; whereas materials without hydrothermal treatment, also showed dehydrogenating activity.

All these results indicate that the main reaction, when CH_3CN is employed as the solvent, develops into the homogeneous phase. The role of the catalyst surface is to modify the selectivity to cyclohexanone as the acidity changes by the hydrotreatment.

3.2.2.6 Oxidizing Agent Effect Figure 12 shows the effect of two different oxidizing agents on the cyclohexanol conversion and cyclohexanone selectivity. There, the oxidizing behaviors of H_2O_2 (30%) and TBHP (70% weight) in water are compared. The amount of the oxidizing agent, in both cases, was the necessary to keep the molar ratio (R) of the substrate to oxidizing agent equal to one. All the other reaction conditions were that described in the "Experimental" section.

After 7 h of reaction, although hydrogen peroxide showed greater activity than TBHP (C_{C-OH} = 60 vs. 25%, respectively), the last one showed a higher selectivity to the carbonyl derivative (up to 55%); the highest from the previously described experiment.

As it was discussed above, H_2O_2 quickly decomposes in the presence of the chromium catalyst, oxidizing the Cr^{3+} to Cr^{6+} who starts the reaction into the homogeneous phase promoting the degradation of the hydrocarbon chain. So, in spite of TBHP is less reactive than H_2O_2 it is more selective to the carbonyl derivative (55%). This behavior probably relates to that the TBHP (70% in H_2O) introduces a smaller amount of water to the reaction medium and explains previous results reported in the bibliography [19] wherein, using a non-aqueous solvent (Cl-benzene) and anhydrous TBHP as the oxidizing agent, selectivity remains close to 90% under mild oxidation conditions.

3.2.3 Verbenol to Verbenone Oxidation

To complement the previous results, we investigate the oxidation of verbenol to verbenone. Like any allylic alcohol, we expected a straightforward oxidation towards the carbonyl derivative. The reaction was carried out, using H_2O_2 (30%) as an oxidizing agent, over the catalyst hydrothermally treated at 150 °C ($5SG_{150}^{110}$), as it is the one with an intermediate activity.

It can be seen (Fig. 13) that verbenol conversion reached 94% after 6 h of reaction with a conversion to verbenone of 53% (selectivity 56%). This selectivity was superior to that obtained with the other cyclic substrates (cyclohexanol, cyclohexene, and cyclohexanone) under the same conditions of reaction. The difference is mainly attributed to that verbenol oxidation to α-β carbonyl derivative is thermodynamically favored, while in the other cyclic compounds, the ring opening is privileged, so the reaction is largely directed towards degradation of the ring.

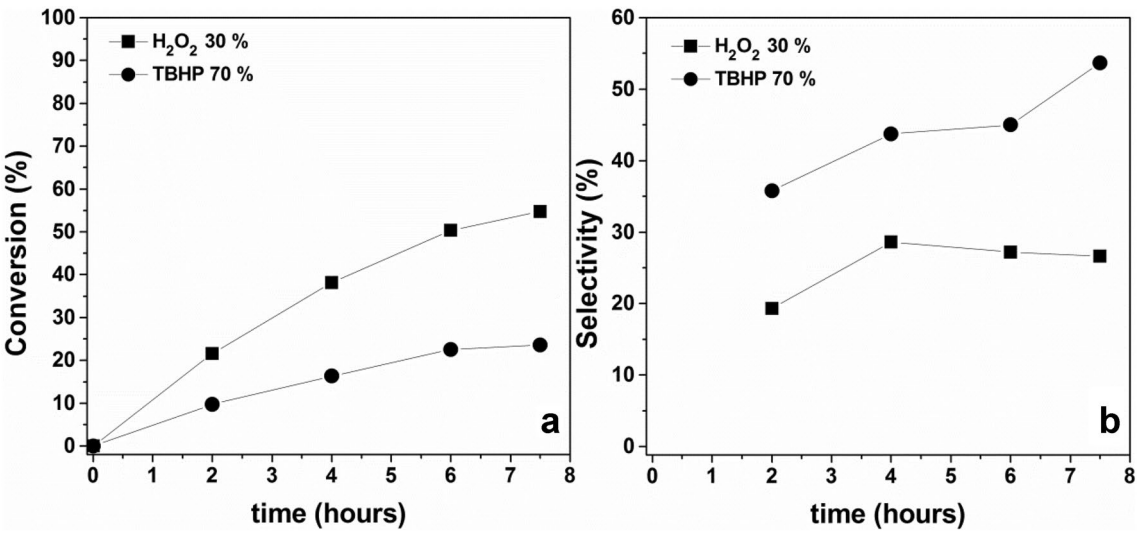

Fig. 12 Oxidizing agent effect on **a** cyclohexanol conversion and **b** cyclohexanone selectivity. Oxidant agents: H_2O_2 (0.7 mL, 30%) and TBHP (0.9 mL, 70%), R (molar ratio substrate/oxidant) = 1. Reaction conditions: Temperature: 70 °C. Solvent: CH_3CN (5 mL). Catalyst: $5SG_{nHT}^{110}$ (10 mg). Substrate: cyclohexanol (0.5 mL)

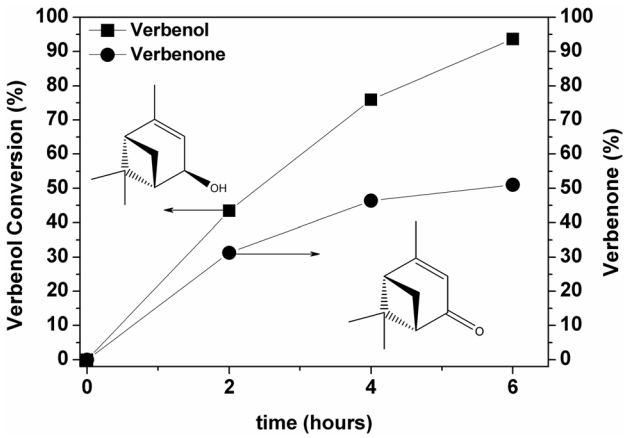

Fig. 13 Verbenol oxidation to verbenone in the presence of H_2O_2 on $5SG_{150}^{110}$ catalyst. Reaction conditions: Temperature: 70 °C. Solvent: CH_3CN (5 mL). Catalyst: $5SG_{150}^{110}$ (10 mg). Substrate: verbenol (0.5 mL). Oxidizing agent: H_2O_2 (0.7 mL, 30%)

4 Conclusions

Cr/SiO_2 in acetonitrile constitutes a catalytic system showing high activity for cyclic hydrocarbons oxidation. The H_2O presence favors the solubility of Cr^{6+} species, conducting the reaction into the liquid phase. Under the general experimental conditions used (70 °C, R = 1 and hydrogen peroxide as an oxidizing agent) the cycle opening and degradation of the hydrocarbon chain was favored.

The oxidation reaction starts, by the hydrogen peroxide decomposition on the catalyst surface, oxidizing Cr^{3+} to Cr^{6+}. The soluble Cr^{6+} peroxides promote, by a free radical mechanism, the oxidation and degradation of the cyclic hydrocarbon in the homogeneous phase. Without the catalyst and after 5 h of reaction, the conversion was almost null, demonstrating the true catalytic behavior of 5SG materials.

By using CH_3CN as a solvent and H_2O_2 as an oxidant, materials show an important leaching process, yielding a high concentration of Cr (VI) species in solution. The leaching process is lower on materials hydrothermally treated at high temperatures.

Using TBHP as an oxidizer, the yield to cyclohexanone improves due to the lower reactivity of TBHP and a lesser solubility of the Cr^{6+} peroxides in this reaction medium whit less water content.

Finally, by replacing cyclohexanol for verbenol, a cyclic allylic alcohol, in the presence of H_2O_2/CH_3CN it was possible to achieve a verbenol conversion near to 95% and selectivity to verbenone around 60%.

Acknowledgements This work was performed under the auspices and the financial support of INIQUI-CONICET and CIUNSa.

Funding Funding was provided by Consejo de Investigación, Universidad Nacional de Salta and Consejo Nacional de Investigaciones Científicas y Técnicas.

Compliance with Ethical Standards

Conflict of interest Authors declare they have not any ethical conflict of interest related to the publication and its content.

References

1. Bellifa A, Choukchou-Braham A, Kappenstein C, Pirault-Roy L (2014) RSC Adv 4:22374
2. Hagen J (2015) Homogeneously catalyzed industrial processes, Wiley, New Jersey
3. Lancaster M (2007) Principles of sustainable and green chemistry, Blackwell Science Ltd, New Jersey
4. Schuchardt U, Cardoso D, Sercheli R, Pereira R, da Cruz RS, Guerreiro MC, Mandelli D, Spinacé EV, Pires EL (2001) Appl Catal A 211:1
5. Taghavimoghaddam J, Knowles GP, Chaffee AL (2012) J Mol Catal A 358:79
6. Sakthivel A, Selvam P (2002) J Catal 211:134
7. Tangale NP, Niphadkar PS, Deshpande SS, Joshi PN (2013) Appl Catal A 467:421
8. Jevtic R, Ramachandran PA, Dudukovic MP (2009) Ind Eng Chem Res 48:7986
9. Rodionova LI, Smirnov AV, Borisova NE, Khrustalev VN, Moiseeva AA, Grünert W (2012) Inorg Chim Acta 392:221
10. Adam F, Retnam P, Iqbal A (2009) Appl Catal A 357:93
11. Schuchardt U, Carvalho WA, Spinacé EV (1993) Synlett 1993, 713
12. Fridman VZ, Davydov AA (2000) J Catal 195:20
13. Romero A, Santos A, Escrig D, Simón (2011) E. Appl Catal A 392:19
14. Sridevi B, Nagaiah P, Padmasri AH, David Raju B, Rama Rao KS (2017) J Chem Sci 129:601
15. Wang Z, Liu X, Rooney DW, Hu P (2015) Surf Sci 640:181
16. da Cruz RS, de Souza e Silva JM, Arnold U, Schuchardt U (2001) J Mol Catal A 171:251
17. Bérubé F, Khadraoui A, Florek J, Kaliaguine S, Kleitz F (2015) J Coll Interface Sci 449:102
18. Samanta S, Mal NK, Bhaumik A (2005) J Mol Catal A 236:7
19. Parentis ML, Bonini NA, Gonzo EE (2002) React Kinet Catal Lett 76:243
20. Sakthivel A, Dapurkar SE, Selvam P (2003) Appl Catal A 246:283
21. Shylesh S, Samuel PP, Singh AP (2007) Appl Catal A 318:128
22. Shylesh S, Srilakshmi C, Singh AP, Anderson BG (2007) Microporous Mesoporous Mater 99:334
23. Lempers HEB, Sheldon RA (1998) J Catal 175:62
24. Laha SC, Gläser R (2007) Microporous Mesoporous Mater 99:159
25. Cuesta Zapata PM, Nazzarro MS, Gonzo EE, Parentis ML, Bonini NA (2016) Catal Today 259:39
26. Cuesta Zapata PM, Nazzarro MS, Parentis ML, Gonzo EE, Bonini NA (2013) Chem Eng Sci 101:374
27. Cuesta Zapata PM, Parentis ML, Gonzo EE, Bonini NA (2013) Appl Catal A 457:26
28. Delley MF, Praveen CS, Borosy AP, Núñez-Zarur F, Comas-Vives A, Copéret C (2017) J Catal 354:223
29. Demmelmaier CA, White RE, van Bokhoven JA, Scott SL (2009) J Catal 262:44

30. Floryan L, Borosy AP, Núñez-Zarur F, Comas-Vives A, Copéret C (2017) J Catal 346:50
31. Huheey JE, Keiter EA, Keiter RL, Medhi OK (2006) Principles of Structure and Reactivity, Pearson Education, New Delhi
32. Vafaeezadeh M, Hashemi MM, Shakourian-Fard M (2012) Catal Commun 26:54
33. Vafaeezadeh M, Mahmoodi Hashemi M (2014) Catal Commun 43:169
34. Won T-J, Lee Y-I (2006) Microchem J 82:73

Affiliations

José Feliciano Miranda[1] · Pablo M. Cuesta Zapata[1] · Elio E. Gonzo[2] · Mónica L. Parentis[2] · Lilian E. Davies[1] · Norberto A. Bonini[1]

José Feliciano Miranda
josefm.86@gmail.com

Pablo M. Cuesta Zapata
pcuesta@unsa.edu.ar

Elio E. Gonzo
gonzo@unsa.edu.ar

Mónica L. Parentis
mparentis@unsa.edu.ar

Lilian E. Davies
lilian@exa.unsa.edu.ar

[1] Facultad de Ciencias Exactas, INIQUI – CONICET, Universidad Nacional de Salta, Avda. Bolivia 5150, 4400 Salta, Argentina

[2] Facultad de Ingeniería, INIQUI – CONICET, Universidad Nacional de Salta, Avda. Bolivia 5150, 4400 Salta, Argentina